

P1.6

A COMPARISON OF SURFACE FLUX PRODUCTS FROM GEWEX SURFACE RADIATION BUDGET WITH ECMWF ERA-40, NCEP/NCAR REANALYSIS AND CERES SRBAVG

J. Colleen Mikovitz^{*1}, Paul W. Stackhouse, Jr.², Shashi K. Gupta¹, Taiping Zhang¹, Stephen J. Cox¹, David R. Doelling¹, Dennis F. Keyes¹ and Laura M. Hinkelman³
¹AS&M, Inc., Hampton, VA, ²NASA/LaRC, Hampton, VA, ³NIA, Hampton, VA

1. INTRODUCTION

The NASA/GEWEX Surface Radiation Budget (SRB) project at NASA Langley Research Center has recently produced a climatology spanning 21.5 years (July 1983 - December 2004) of shortwave (SW) and longwave (LW) radiative flux products. SRB estimates surface and top-of-atmosphere (TOA) radiative flux quantities using satellite observations, re-analysis meteorology, and ozone as inputs to parameterized radiation models. In this paper, monthly averaged SRB flux products are compared with similar products available from the European Centre for Medium-Range Weather Forecasts (ECMWF) 40-year data set (ERA-40), NCEP/NCAR Reanalysis (NCEP) and the Clouds and the Earth's Radiant Energy System (CERES) surface radiation budget average (SRBAVG) for the period from March 2000 through February 2003. Both surface and TOA fluxes are compared. Select meteorological inputs to the algorithms will also be discussed and related to the flux differences. Global and zonal maps of selected months illustrate the extent of differences that will be taken as an indication of how the uncertainty in the meteorological fields affects the resulting fluxes. Finally, the fluxes from SRB will be validated against high quality measurements taken from surface sites of the Baseline Surface Radiation Network (BSRN). These results will have implications regarding the uncertainties limiting the estimate of surface fluxes.

2. DATA SET DESCRIPTION

The SW flux products from SRB are produced using an adaptation of the Pinker/Laszlo shortwave algorithm (Pinker and Laszlo 1992),

**Corresponding author address:* Colleen Mikovitz, Analytical Services & Materials, Inc., One Enterprise Pkwy., Suite 300, Hampton, VA 23666. E-mail: j.c.mikovitz@larc.nasa.gov

while the LW flux products are generated by an adaptation of the Fu et al. (1997) thermal infrared radiative transfer code.

Inputs to the SRB flux algorithms include cloud properties derived from International Satellite Cloud Climatology Project (ISCCP) pixel level (DX) data (Rossow and Schiffer 1999), temperature and humidity profiles from Goddard Earth Observing System version 4.0.3 (GEOS-4) long-term meteorological reanalysis (Bloom et al. 2005) and column ozone from TOMS and TOVS archives.

Monthly flux products from the NCEP/NCAR Reanalysis (Kalnay et al. 1996) are available as a subset of the original 4 times daily data assimilation. These data are available online from 1948 up to the present. Flux products for ERA-40 are available from 1957 through 2002 online. Because of this, comparisons with ERA-40 will be limited by the shorter time period. Both of these reanalysis products are available on a $2.5^\circ \times 2.5^\circ$ grid. Doelling et al. (2006) are presenting a description of the CERES SRBAVG products at this conference. TOA fluxes used here are the CERES/geostationary (GEO) data. For this work, all parameter comparisons were accomplished on $1^\circ \times 1^\circ$ resolution grid.

3. RESULTS

a. Outgoing Longwave Radiation

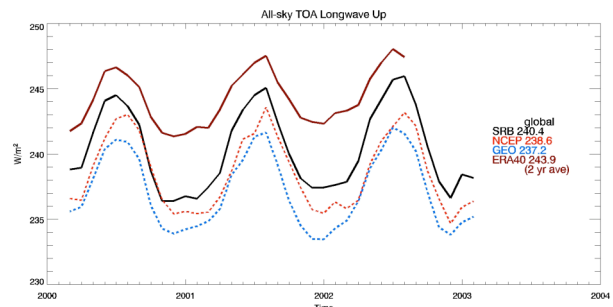


Fig. 1. Global monthly averaged time series of OLR for Mar 2000 – Feb 2003.

The time series of outgoing longwave radiation (OLR) global averages in Fig. 1 shows

relatively good agreement between all algorithms. With the exception of ERA-40, the models are within 5 Wm^{-2} of the CERES GEO global average across the three years.

A time-latitude cross-section of differences between SRB and CERES GEO (Fig. 2) illustrate typical patterns of differences. SRB is mostly within 10 Wm^{-2} . Larger differences occur in mostly desert regions in Africa and the Middle East, but are smoothed by the averaging.

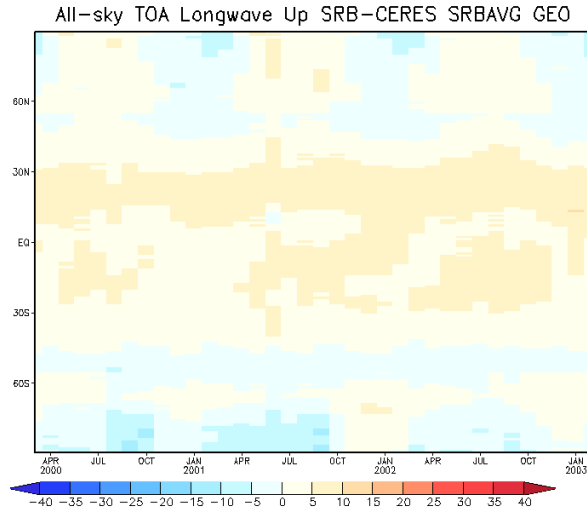


Fig. 2. Time-latitude cross-section difference of OLR for Mar 2000 - Feb 2003: SRB-CERES GEO

A sample map of the differences between SRB and ERA-40 and a time-latitude cross-section of the differences between SRB and NCEP are shown in Figs. 3 and 4. In these, the largest feature seems to be related to the ITCZ position. Pole-ward from 30° in each hemisphere, ERA-40 has consistently higher OLR fluxes than SRB.

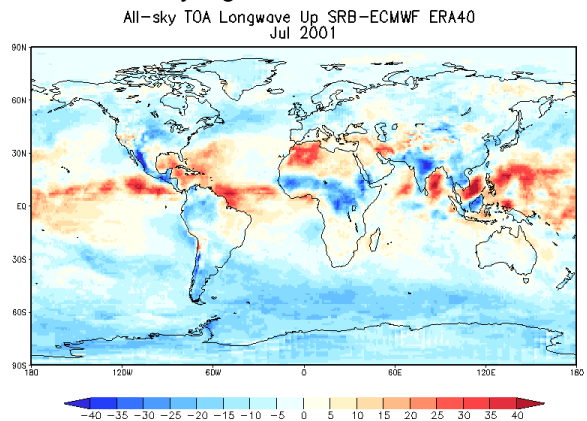


Fig. 3. Monthly averaged OLR difference for July 2001: SRB-ERA40

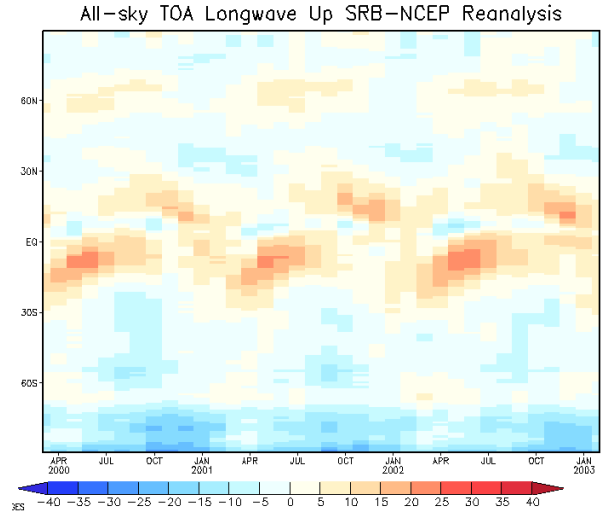


Fig. 4. Time-latitude cross-section difference of OLR for Mar 2000 - Feb 2003: SRB-NCEP

b. TOA Reflected Shortwave Flux

The global time series of TOA reflected SW flux is shown in Fig. 5. SRB mirrors CERES GEO quite well for the time series, with the global difference being within 3.5 Wm^{-2} . The NCEP global average is almost 20 Wm^{-2} larger than CERES GEO. ERA-40 data is unavailable from the website for this parameter.

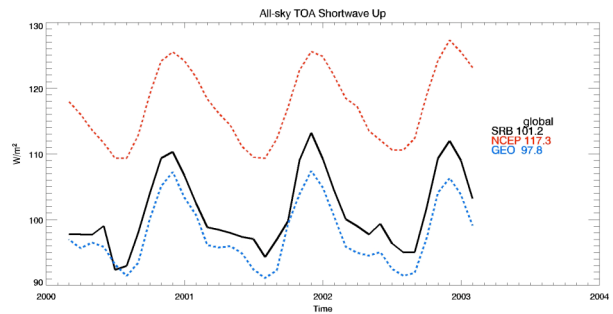


Fig. 5. Global monthly averaged time series of TOA reflected SW for Mar 2000 - Feb 2003.

A map of the differences between SRB and CERES GEO for July 2001 is shown in Fig. 6. Reflected SW differences are generally small, with largest differences at high latitudes during the summer. The time-latitude cross-section of the difference between SRB and NCEP in Fig. 7 shows that the tropics are a major source of the large global difference in the reflected SW. Upon inspection of map differences (not shown), the positive differences in the higher latitudes during

the respective summers occur mostly along coastlines.

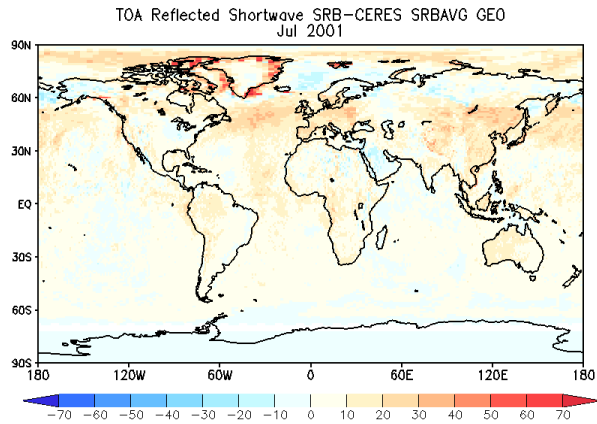


Fig. 6. Monthly averaged TOA reflected SW difference for July 2001: SRB-CERES GEO

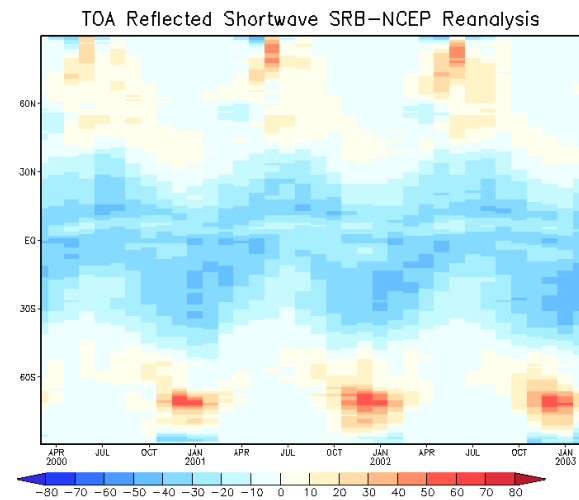


Fig. 7. Time-latitude cross-section difference of TOA reflected SW for Mar 2000 - Feb 2003: SRB-NCEP

c. Surface Shortwave Net Flux

As seen in the time series of surface SW net flux (Fig. 8), the global average of SRB lies in the middle of the range of the models. CERES SRBAVG is highest throughout the time, higher than SRB by about 10 Wm^{-2} . ERA-40 is lower than SRB by 10 Wm^{-2} . NCEP and SRB are similar in the time series, differing by about 2 Wm^{-2} .

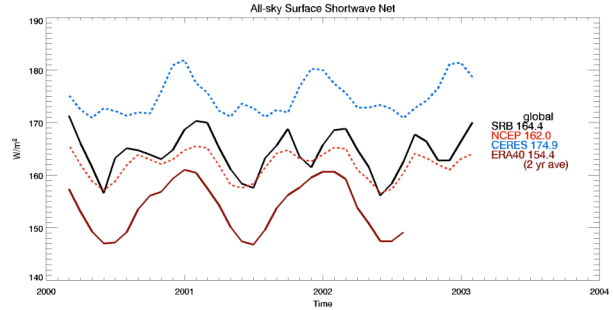


Fig. 8. Global monthly averaged time series of surface SW net for Mar 2000 - Feb 2003.

The January 2001 map (Fig. 9) of the differences between SRB and CERES SRBAVG illustrate that, in general, the lower net fluxes of SRB are present everywhere. Exceptions occur at the edge of the geostationary satellite boundaries. This pattern persists through the time period of study, although with some seasonal dependence of the magnitude of the difference.

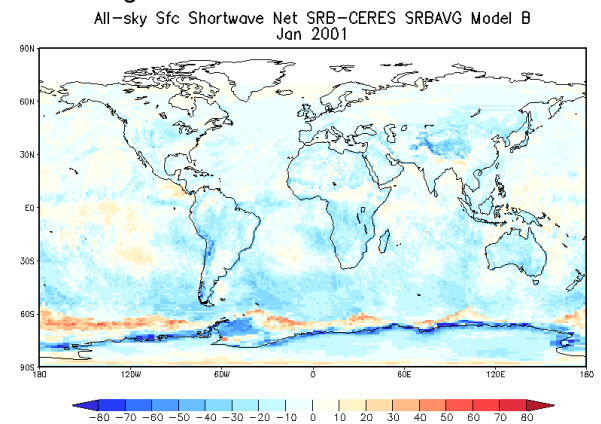


Fig. 9. Monthly averaged surface SW net difference for Jan 2001: SRB-CERES Model B

The patterns of differences with SRB of the SW net between NCEP and ERA-40 are similar. The difference with NCEP is shown in the time-latitude cross-section, Fig. 10. In the tropics, SRB has higher net fluxes, while during summer in the Polar regions, the net flux is smaller. The magnitude of these differences can be as large as 40 Wm^{-2} . This pattern of negative and positive differences, particularly with NCEP, leads to the overall small bias in global averages.

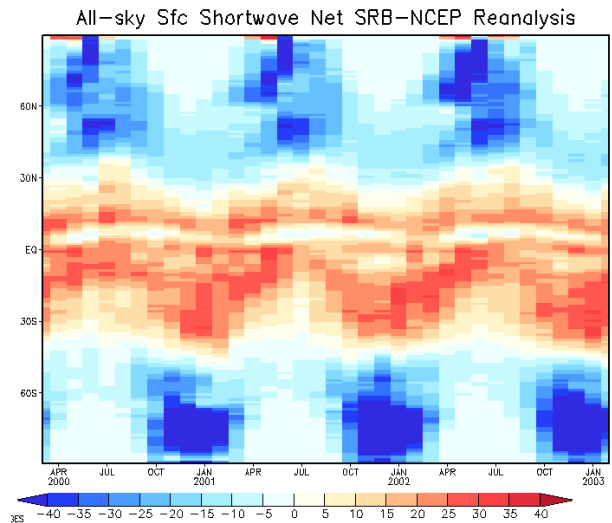


Fig. 10. Time-latitude cross-section difference of surface SW net for Mar 2000 - Feb 2003: SRB-NCEP

d. Surface Longwave Net Flux

The global average time series of surface LW net flux (Fig. 11) shows SRB in the middle of the range of all models. The SRB global average is within 1 Wm^{-2} of ERA-40's average and within 10 Wm^{-2} from NCEP and CERES SRBAVG.

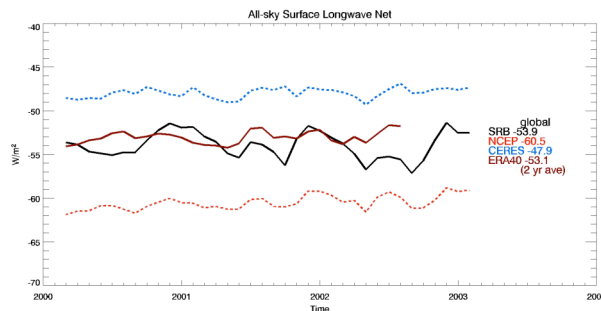


Fig. 11. Global monthly averaged time series of surface LW net for Mar 2000 - Feb 2003.

Much of the global average difference between SRB and NCEP arises from the winter season at the Poles, as seen in Fig. 12, while most other places, especially Africa and the Middle East contribute to a difference in the net flux of the opposite sign. Many of these flux differences can be explained by skin temperature differences, as will be seen in section e.

The seasonal nature of the differences can be seen clearly in the time-latitude cross-sections. The patterns of the differences are similar for all model/product comparisons with SRB. A sample with ERA-40 is shown in Fig. 13. Note that ERA-40 is only available through August 2002. CERES

SRBAVG has lower magnitude differences with SRB at the Poles, while higher over Africa. NCEP has higher magnitude differences at the Poles.

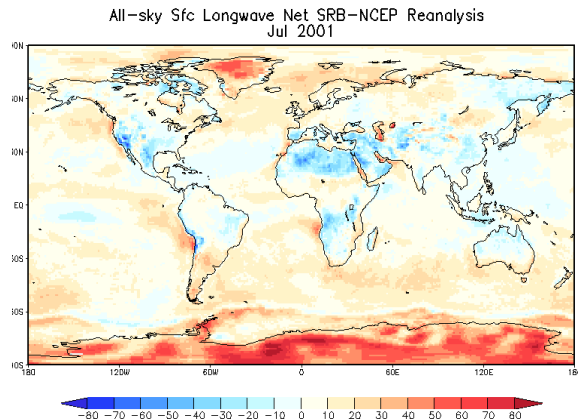


Fig. 12. Monthly averaged surface LW net difference for July 2001: SRB-NCEP

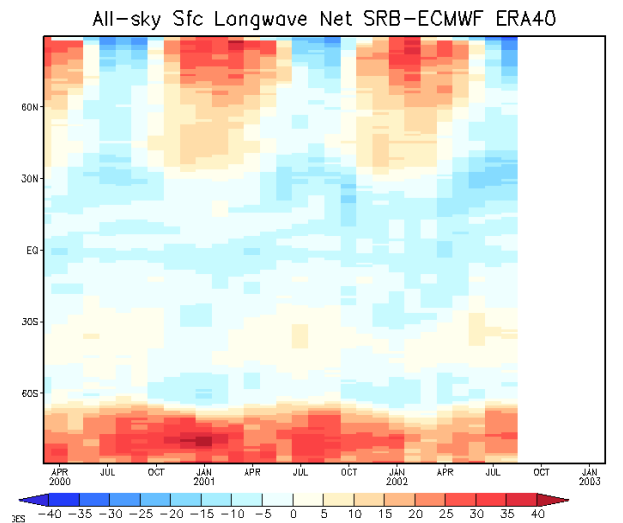


Fig. 13. Time-latitude cross-section difference of surface LW net for Mar 2000 - Aug 2002: SRB-ERA40

e. Meteorological Parameters

The quality of meteorological inputs to models is important to the outcome of the model fluxes. Skin temperature is especially important to surface longwave fluxes. For this study, only access to NCEP skin temperature was possible.

Skin temperature input into SRB algorithms comes from GEOS-4. A global and tropical time series of skin temperature is presented in Fig. 14. For the global series, NCEP has a smaller range in the annual cycle, while the global average is only 0.1 K smaller than SRB. SRB has a consistent 0.6 K bias in the tropics.

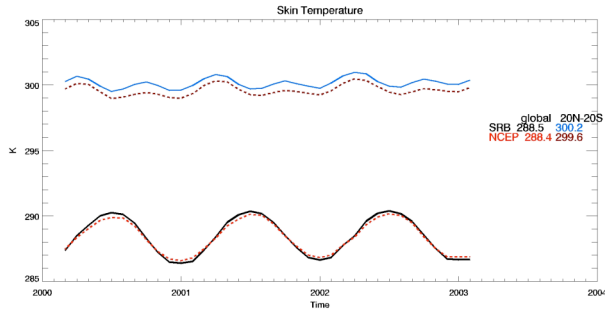


Fig. 14. Global and tropical monthly averaged time series of surface skin temperature for Mar 2000 – Feb 2003.

The map difference for July 2001 (Fig. 15) shows the regional variations that are present throughout the year, for the most part. The Northern Hemisphere has slightly more seasonal variation in the differences, with SRB having smaller temperatures over mid-latitude land areas during the winter. These skin temperature differences directly affect surface LW upward flux, which is a component of the surface LW net flux. Patterns of the opposite sign emerge in the LW net flux difference seen in Fig. 12.

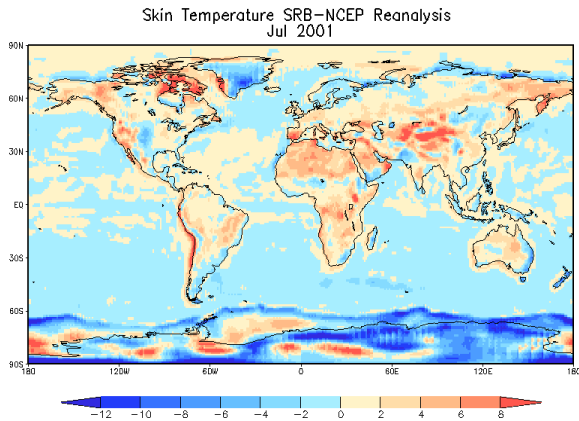


Fig. 15. Monthly averaged surface skin temperature difference for July 2001: SRB-NCEP

Total column precipitable water is also available from NCEP. Precipitable water for SRB is calculated by integrating the moisture profiles from GEOS-4. Global and tropical time series are presented in Fig. 16. As seen in this figure and in the map differences from July 2001 (Fig. 17), the largest differences are in the tropics, although the highest precipitable water values are present there.

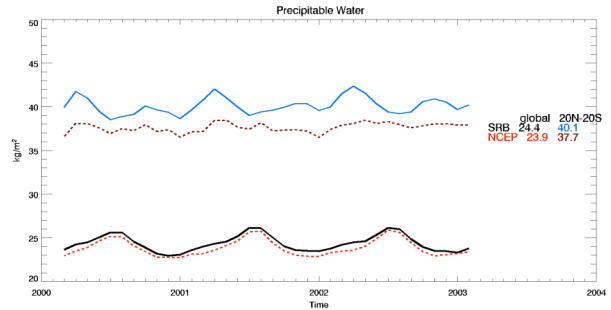


Fig. 16. Global and tropical monthly averaged time series of total column precipitable water for Mar 2000 – Feb 2003.

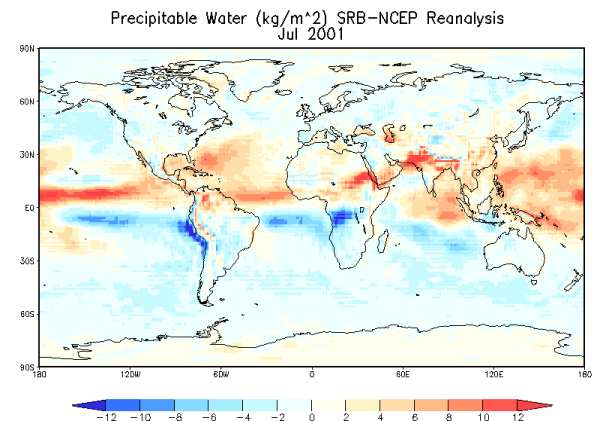


Fig. 17. Monthly averaged total column precipitable water difference for July 2001: SRB-NCEP

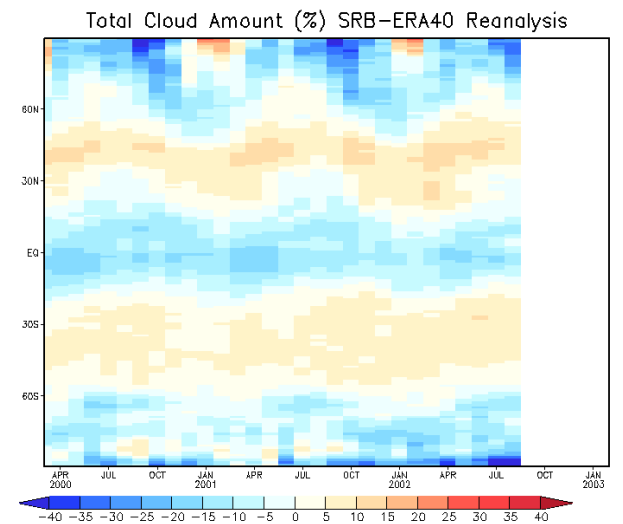


Fig. 18. Time-latitude cross-section difference of total cloud amount for Mar 2000 – Aug 2002: SRB-ERA40

Cloud amount differences between ERA-40 and SRB (from ISCCP DX) are presented in Fig.

18. Typically SRB has fewer clouds in the tropics and Polar regions, and more clouds in the mid-latitudes. There are regional and seasonal differences beyond these trends.

The effect of cloud amount differences on the flux differences can be seen, for example, by comparing the map of cloud amount differences in Fig. 19 with the OLR difference map of Fig. 3. Notice the higher SRB flux in the Western Pacific corresponding to the lower cloud amounts.

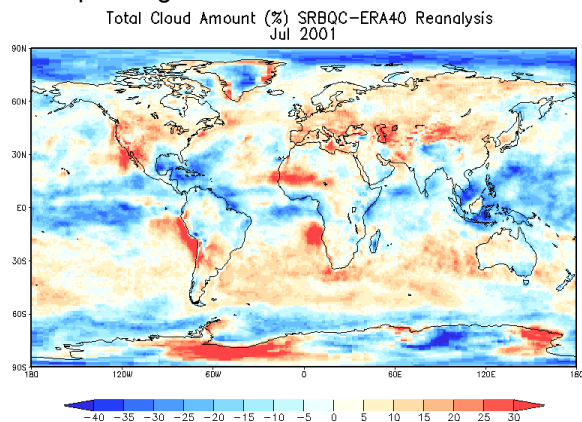


Fig. 19. Monthly averaged total cloud amount difference for July 2001: SRB-ERA40

f. Surface Validation

Surface validation of LW and SW downward fluxes is accomplished by using the BSRN observations from 30 sites. These components were unavailable for NCEP. Results of the validation are presented in Tables 1 and 2. Because ERA-40 ends with August 2002, the number of comparisons with surface observations is smaller, thus the mean of the observations is different. SRB has the highest magnitude bias for SW, with a value of -9.0 Wm^{-2} . CERES Model B has the lowest bias at 2.98 Wm^{-2} . SRB has the middle value for the remainder of the statistics for SW compared with CERES and ERA-40.

LW validation shows all three products compare well with the surface observations. Bias values are all within 1.5 Wm^{-2} . Root mean square differences and standard deviations are well under 15 Wm^{-2} .

Table 1. Comparative statistics for surface SW down

SW down	N	Bias	St. Dev	RMS	Corr. coeff	Mean obs
SRB	813	-9.00	18.78	20.81	0.975	187.33
CERES	813	2.98	16.70	16.96	0.980	187.33
ERA40	692	-4.94	22.70	23.22	0.961	193.44

Table 2. Comparative statistics for surface LW down

LW down	N	Bias	St. Dev	RMS	Corr. coeff	Mean obs
SRB	756	-0.95	13.00	13.03	0.983	310.34
CERES	756	1.36	10.74	10.82	0.988	310.34
ERA40	637	-1.01	11.61	11.64	0.989	311.81

4. CONCLUSIONS

This paper has shown that despite the varied inputs into the models and assimilations, the results are quite comparable on a global analysis. Time series comparisons of global averages are rarely far off from each other. Regional differences, however, can be quite large, as seen in the various maps of differences. Known limitations of inputs (e.g. skin temperature values at the Poles) can improve understanding of the differences in fluxes.

ACKNOWLEDGEMENTS

Funding was provided under NASA grant MDAR-0506-0383 under the EOS Interdisciplinary Science program (NRA-99-OES-04).

REFERENCES

- Bloom, S., A. da Silva, D. Dee, M. Bosilovich, J-D. Chern, S. Pawson, S. Schubert, M. Sienkiewicz, I. Stanjer, W-W. Tan, and M-L. Wu, 2005: Documentation and validation of the Goddard Earth Observing System (GEOS) Data Assimilation System – Version 4. *NASA/TM-2005-104606*, Vol. 26, 187 pp.
- Doelling, D., D. F. Young, B. A. Wielicki, T. Wong and D. F. Keyes, 2006: The newly released 5-year Terra-based monthly CERES radiative flux and cloud product. AMS 12th Conference on Atmospheric Radiation.
- Fu, Q., K. N. Liou, and A. Grossman, 1997: Multiple scattering parameterization in thermal infrared radiative transfer. *J. Atmos. Sci.*, **54**, 2799-2814.
- Kalnay, E. and Coauthors, 1996: The NCEP/NCAR 40-Year Reanalysis Project. *Bull. Amer. Meteor. Soc.*, **77**, 437-471.

Pinker, R., and I. Laszlo, 1992: Modeling surface solar irradiance for satellite applications on a global scale. *J. Appl. Meteor.*, **31**, 194-211.

Rossow, W. B., and R. A. Schiffer, 1999: Advances in understanding clouds from ISCCP. *Bull. Amer. Meteor. Soc.*, **80**, 2261-2287.